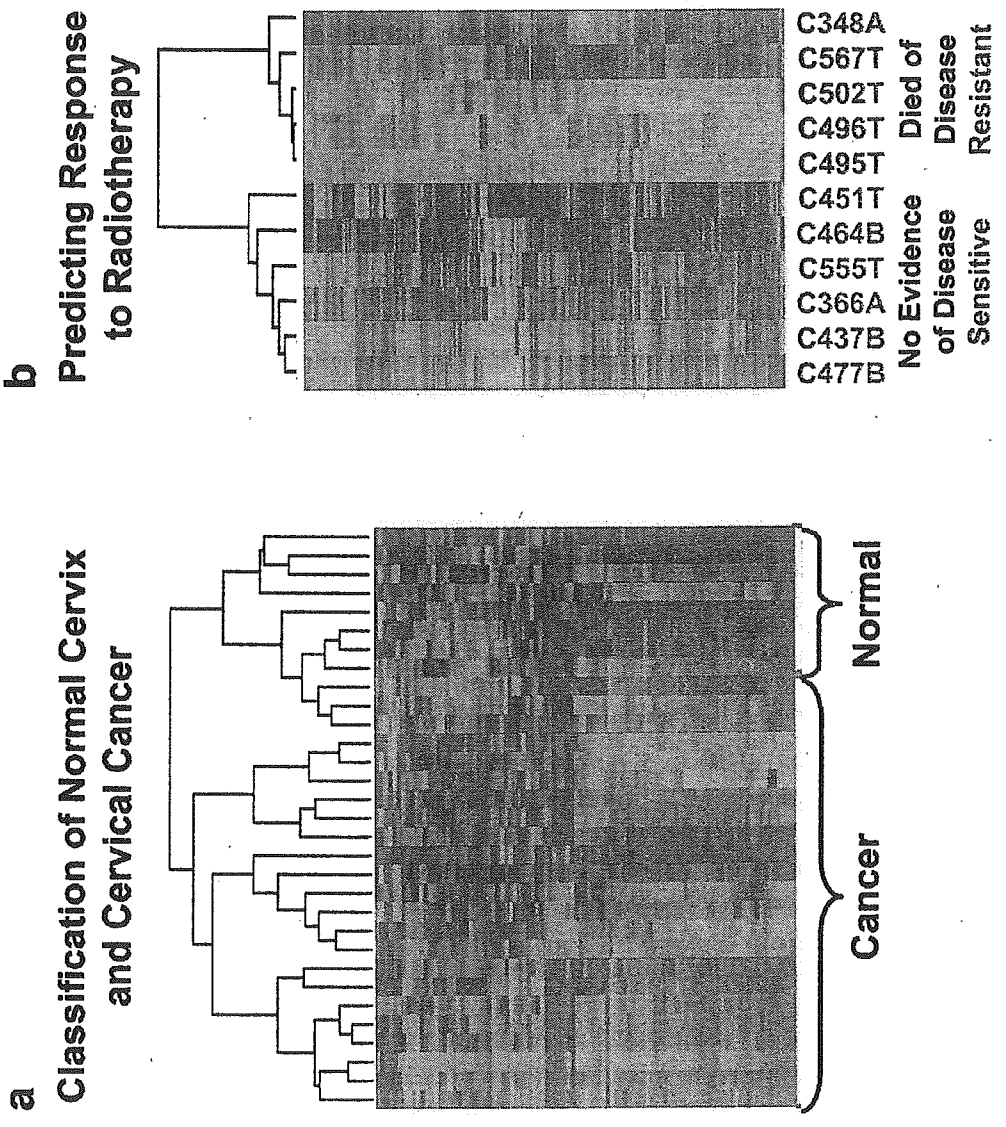

FIGURE 1. *See following page for legend.*

scripts or genes. We first assessed the suitability of voice/speech pattern recognition algorithm for gene expression data analysis by testing whether the process can distinguish the expression profiles of normal cervices derived from hysterectomy from cervical cancer samples. A pattern recognition algorithm classified all the samples correctly as either normal or cancer based on their gene expression data (FIG. 1a).

Cervical cancer is pathologically staged into four stages according to the FIGO system. We next showed by pattern recognition that a subset of the cancer samples in our study can be correctly classified into either Stage IB or Stage IIB. Together, these and the above results suggest that the voice/speech pattern recognition approach can be used for gene expression data analysis.

The patients in our study were given radiotherapy as primary treatment and were further stratified into two groups: radiotherapeutic sensitive (responder) or resistance (nonresponder). The clinical data indicated that patients who did not respond to radiotherapy had a mean survival time of 22.2 months, while the group who responded had a mean survival time of 66.5 months. Voice/speech pattern recognition analysis correctly classified the samples as either radiotherapy-sensitive or radiotherapy-resistant based on their gene expression profiles (FIG. 1b).

By this analysis, the signature expression profile correctly predicted the patients' response to radiotherapy. These signature predictors were made up of a set of genes with diverse physiologic functions, which include transcription factors, proteins with cytoskeletal, membrane and cell structural functions. Bioinformatics searches of these predictors did not reveal insights into their roles in modulating cellular sensitivity or resistance to radiation therapy. In addition, further analysis of a larger cohort of cervical cancer patients treated by radiotherapy will be required to confirm the signature predictors and to determine the role of these genes in modulating response to radiotherapy.

Predicting Response to Chemotherapy

In ovarian cancer, emergence of drug resistance during chemotherapy results in death for more than 90% of patients with metastatic disease. The poor prognosis has prompted major efforts to identify prognostic factors, improve surgical staging, and develop adjuvant therapies that could improve patient outcome.[43] The above analysis examined cervical cancer patients given only radiation treatment. To test whether treatment response can be predicted in a more complex treatment model, we examined the expression profiles of primary ovarian cancer samples from patients given a platinum-based combination chemotherapeutic regimen of either Cisplatin/ cyclophosphamide, or Carboplatin/taxol, or Cisplatin/taxol. Patients were stratified into two groups based on their chemotherapeutic response.[39]

Pattern recognition analysis of the transcription profiles of the ovarian cancer samples generated a signature predictor set that correctly predicted the response of

---

FIGURE 1. Transcription profiling of cervical cancer. **a**, Molecular classification of cervical cancer by DNA microarray. Normal cervix and cervical cancer samples were correctly classified by voice/speech/pattern recognition. **b**, Prediction of radiotherapy response in cervical cancer based on transcription profiles of primary cervical cancer samples obtained at time of diagnosis before therapy was given.

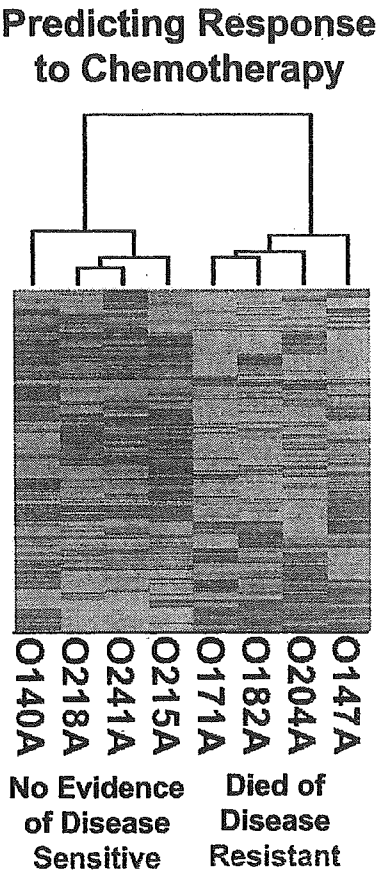

	Treatment
O147A	Cisplatin/Cyclophosphamide
O204A	Cisplatin/Cyclophosphamide
O182A	Cisplatin/Cyclophosphamide
O171A	Cisplatin/Taxol
O215A	Carboplatin/Taxol
O241A	Carboplatin/Taxol
O218A	Cisplatin/Cyclophosphamide
O140A	Cisplatin/Cyclophosphamide

FIGURE 2. Predicting response to chemotherapy in ovarian cancer. Pattern matching algorithm correctly predicted treatment response and the displayed dendrogram showed patients who either responded to or failed the given treatment regimens.

the two groups of patients as either chemotherapy sensitive or chemotherapy resistant (FIG. 2).

In this signature predictor set, we observed an increase in glutathione S-transferase expression, which is well known to confer increased resistance to Cisplatin.[29] Further examination of some of these predictor genes reveals a cluster of transcription or protein factors that bind DNA, whose expression are increased in the cancer samples of patients who did not respond to treatment. This signature expression pattern is reminiscent of the expression profiles found in ovarian cancer cell lines exposed to Cisplatin in temporal gene expression studies (unpublished data), thus suggesting that these nucleic acid binding proteins may have an important biologic role in conferring either intrinsic or acquired drug resistance in ovarian cancer. Whether the transcriptional changes in the expression of these predictor genes are associated with the etiologic causes of drug resistance or treatment failure in ovarian cancer given the above combination platinum-based therapies remains to be determined in future studies with a larger cohort of patients. Nevertheless, these proof-of-principle studies provided support that gene-expression profiling analysis is suited for the molecular classification of cancer and prediction of treatment response.

EPILOGUE

Monitoring gene expression profiles by DNA microarray in human cancer as well as other diseases will be the gateway genomic approach to diagnosis, which will provide pharmacogenomics information for molecular classification of diseases and predict susceptibility to drug toxicity and treatment outcome. Transcription profiling has already been increasingly used in studying human cancer samples for predicting treatment response and disease outcome.[40,44–53] This approach will undoubtedly bring an end to the trial and error and one-size-fits-all medical practice in the treatment of cancer and other human diseases. Patients whose expression profiles exhibit pattern associated with resistance to treatment will be given alternative or supplementary modality of treatment that may result in improved responsiveness or cure, thus personalizing treatment for individuals based on their gene expression patterns.

[*Competing interests statement:* The authors state that they have no competing financial interests.]

REFERENCES

1. CHIN, K.V., I. PASTAN & M.M. GOTTESMAN. 1993. Function and regulation of the human multidrug resistance gene. Adv. Cancer Res. **60:** 157–180.
2. HAFFTY, B.G. & P.M. GLAZER. 2003. Molecular markers in clinical radiation oncology. Oncogene **22:** 5915–5925.
3. MARTIN, N.M. 2001. DNA repair inhibition and cancer therapy. J. Photochem. Photobiol. B **63:** 162–170.
4. AMBUDKAR, S.V., C. KIMCHI-SARFATY, Z.E. SAUNA & M.M. GOTTESMAN. 2003. P-glycoprotein: from genomics to mechanism. Oncogene **22:** 7468–7485.
5. JULIANO, R.L. & V. LING. 1976. A surface glycoprotein modulating drug permeability in Chinese hamster ovary cell mutants. Biochim. Biophys. Acta **455:** 152–162.
6. KARTNER, N., J.R. RIORDAN & V. LING. 1983. Cell surface P-glycoprotein associated with multidrug resistance in mammalian cell lines. Science **221:** 1285–1288.
7. GOTTESMAN, M.M., T. FOJO & S.E. BATES. 2002. Multidrug resistance in cancer: role of ATP-dependent transporters. Nat. Rev. Cancer **2:** 48–58.
8. BAIRD, R.D. & S.B. KAYE. 2003. Drug resistance reversal—are we getting closer? Eur. J. Cancer **39:** 2450–2461.
9. KAWASE, M. & N. MOTOHASHI. 2003. New multidrug resistance reversal agents. Curr. Drug Targets **4:** 31–43.
10. ROBERT, J. & C. JARRY. 2003. Multidrug resistance reversal agents. J. Med. Chem. **46:** 4805–4817.
11. KELLEN, J.A. 2003. The reversal of multidrug resistance: an update. J. Exp. Ther. Oncol. **3:** 5–13.
12. BATES, S.F., C. CHEN, R. ROBEY, *et al.* 2002. Reversal of multidrug resistance: lessons from clinical oncology. Novartis Found. Symp. **243:** 83–96; discussion, 96–102, 180–105.
13. VOLM, M. 1998. Multidrug resistance and its reversal. Anticancer Res. **18:** 2905–2917.
14. DEAN, M., T. FOJO & S. BATES. 2005. Tumour stem cells and drug resistance. Nat. Rev. Cancer **5:** 275–284.
15. HIROSE, M., E. HOSOI, S. HAMANO & A. JALILI. 2003. Multidrug resistance in hematological malignancy. J. Med. Invest. **50:** 126–135.
16. CHIN, K.V., Z.E. SELVANAYAGAM, R. VITTAL, *et al.* 2004. Application of expression genomics in drug development and genomic medicine. Drug Dev. Res. **62:** 124–133.
17. RAVATN, R., V. WELLS, L. NELSON, *et al.* 2005. Circumventing multidrug resistance in cancer by beta-galactoside binding protein, an antiproliferative cytokine. Cancer Res. **65:** 1631–1634.

18. TLSTY, T.D., Y.G. CRAWFORD, C.R. HOLST, *et al.* 2004. Genetic and epigenetic changes in mammary epithelial cells may mimic early events in carcinogenesis. J. Mammary Gland Biol. Neoplasia **9:** 263–274.
19. MICHOR, F., Y. IWASA, B. VOGELSTEIN, *et al.* 2005. Can chromosomal instability initiate tumorigenesis? Semin. Cancer Biol. **15:** 43–49.
20. RANGARAJAN, A. & R.A. WEINBERG. 2003. Opinion: comparative biology of mouse versus human cells: modelling human cancer in mice. Nat. Rev. Cancer **3:** 952–959.
21. CLEATOR, S., M. PARTON & M. DOWSETT. 2002. The biology of neoadjuvant chemotherapy for breast cancer. Endocrinol. Relat. Cancer **9:** 183–195.
22. XIA, F. & S.N. POWELL. 2002. The molecular basis of radiosensitivity and chemosensitivity in the treatment of breast cancer. Semin. Radiat. Oncol. **12:** 296–304.
23. PERONA, R. & I. SANCHEZ-PEREZ. 2004. Control of oncogenesis and cancer therapy resistance. Br. J. Cancer **90:** 573–577.
24. KUDOH, K., M. RAMANNA, R. RAVATN, *et al.* 2000. Monitoring the expression profiles of doxorubicin-induced and doxorubicin-resistant cancer cells by cDNA microarray. Cancer Res. **60:** 4161–4166.
25. DOHERTY, M.M. & M. MICHAEL. 2003. Tumoral drug metabolism: perspectives and therapeutic implications. Curr. Drug Metab. **4:** 131–149.
26. LIEM, A.A., M.P. CHAMBERLAIN, C.R. WOLF & A.M. THOMPSON. 2002. The role of signal transduction in cancer treatment and drug resistance. Eur. J. Surg. Oncol. **28:** 679–684.
27. SCHMITT, C.A. & S.W. LOWE. 2002. Apoptosis and chemoresistance in transgenic cancer models. J. Mol. Med. **80:** 137–146.
28. TSURUO, T., M. NAITO, A. TOMIDA, *et al.* 2003. Molecular targeting therapy of cancer: drug resistance, apoptosis and survival signal. Cancer Sci. **94:** 15–21.
29. JOSHI, M.B., Y. SHIROTA, K.D. DANENBERG, *et al.* 2005. High gene expression of TS1, GSTP1, and ERCC1 are risk factors for survival in patients treated with trimodality therapy for esophageal cancer. Clin. Cancer Res. **11:** 2215–2221.
30. LANDER, E.S., L.M. LINTON, B. BIRREN, *et al.* 2001. Initial sequencing and analysis of the human genome. Nature **409:** 860–921.
31. VENTER, J.C., M.D. ADAMS, E.W. MYERS, *et al.* 2001. The sequence of the human genome. Science **291:** 1304–1351.
32. PEASE, A.C., D. SOLAS, E.J. SULLIVAN, *et al.* 1994. Light-generated oligonucleotide arrays for rapid DNA sequence analysis. Proc. Natl. Acad. Sci. USA **91:** 5022–5026.
33. SCHENA, M., D. SHALON, R.W. DAVIS & P.O. BROWN. 1995. Quantitative monitoring of gene expression patterns with a complementary DNA microarray. Science **270:** 467–470.
34. SHYAMSUNDAR, R., Y.H. KIM, J.P. HIGGINS, *et al.* 2005. A DNA microarray survey of gene expression in normal human tissues. Genome Biol. **6:** R22.
35. SULTMANN, H. & A. POUSTKA. 2004. Recent advances in transcription profiling of human cancer. Curr. Opin. Mol. Ther. **6:** 593–599.
36. HOOD, L. 2003. Systems biology: integrating technology, biology, and computation. Mech. Ageing Dev. **124:** 9–16.
37. IDEKER, T., T. GALITSKI & L. HOOD. 2001. A new approach to decoding life: systems biology. Annu. Rev. Genomics Hum. Genet. **2:** 343–372.
38. WESTON, A.D. & L. HOOD. 2004. Systems biology, proteomics, and the future of health care: toward predictive, preventative, and personalized medicine. J. Proteome Res. **3:** 179–196.
39. SELVANAYAGAM, Z.E., T.H. CHEUNG, N. WEI, *et al.* 2004. Prediction of chemotherapeutic response in ovarian cancer with DNA microarray expression profiling. Cancer Genet. Cytogenet. **154:** 63–66.
40. WONG, Y.F., Z.E. SELVANAYAGAM, N. WEI, *et al.* 2003. Expression genomics of cervical cancer: molecular classification and prediction of radiotherapy response by DNA microarray. Clin. Cancer Res. **9:** 5486–5492.
41. MERTENS, B.J. 2003. Microarrays, pattern recognition and exploratory data analysis. Stat. Med. **22:** 1879–1899.
42. PAN, W. 2002. A comparative review of statistical methods for discovering differentially expressed genes in replicated microarray experiments. Bioinformatics **18:** 546–554.

43. OZOLS, R.F. 2000. Management of advanced ovarian cancer consensus summary. Advanced Ovarian Cancer Consensus Faculty. Semin. Oncol. **27:** 47–49.
44. ALIZADEH, A.A., M.B. EISEN, R.E. DAVIS, *et al.* 2000. Distinct types of diffuse large B-cell lymphoma identified by gene expression profiling. Nature **403:** 503–511.
45. BEER, D.G., S.L. KARDIA, C.C. HUANG, *et al.* 2002. Gene-expression profiles predict survival of patients with lung adenocarcinoma. Nat. Med. **8:** 816–824.
46. GOLUB, T.R., D.K. SLONIM, P. TAMAYO, *et al.* 1999. Molecular classification of cancer: class discovery and class prediction by gene expression monitoring. Science **286:** 531–537.
47. OCHI, K., Y. DAIGO, T. KATAGIRI, *et al.* 2004. Prediction of response to neoadjuvant chemotherapy for osteosarcoma by gene-expression profiles. Int. J. Oncol. **24:** 647–655.
48. ROSENWALD, A., G. WRIGHT, W.C. CHAN, *et al.* 2002. The use of molecular profiling to predict survival after chemotherapy for diffuse large-B-cell lymphoma. N. Engl. J. Med. **346:** 1937–1947.
49. VAN 'T VEER, L.J., H. DAI, M.J. VAN DE VIJVER, *et al.* 2002. Gene expression profiling predicts clinical outcome of breast cancer. Nature **415:** 530–536.
50. VAN DE VIJVER, M.J., Y.D. HE, L.J. VAN'T VEER, *et al.* 2002. A gene-expression signature as a predictor of survival in breast cancer. N. Engl. J. Med. **347:** 1999–2009.
51. KANETA, Y., Y. KAGAMI, T. KATAGIRI, *et al.* 2002. Prediction of sensitivity to STI571 among chronic myeloid leukemia patients by genome-wide cDNA microarray analysis. Jpn. J. Cancer Res. **93:** 849–856.
52. OKUTSU, J., T. TSUNODA, Y. KANETA, *et al.* 2002. Prediction of chemosensitivity for patients with acute myeloid leukemia, according to expression levels of 28 genes selected by genome-wide complementary DNA microarray analysis. Mol. Cancer Ther. **1:** 1035–1042.
53. KITAHARA, O., T. KATAGIRI, T. TSUNODA, *et al.* 2002. Classification of sensitivity or resistance of cervical cancers to ionizing radiation according to expression profiles of 62 genes selected by cDNA microarray analysis. Neoplasia **4:** 295–303.

Gene Therapy (2005), 1–9

www.nature.com/gt

RESEARCH ARTICLE

Prime-boost vaccination with plasmid DNA and a chimeric adenovirus type 5 vector with type 35 fiber induces protective immunity against HIV

K-Q Xin[1], N Jounai[1], K Someya[2], K Honma[3], H Mizuguchi[4], S Naganawa[5], K Kitamura[5], T Hayakawa[4], S Saha[1], F Takeshita[1], K Okuda[3], M Honda[2], DM Klinman[6] and K Okuda[1]

[1]*Department of Molecular Biodefense Research, Yokohama City University, Graduate School of Medicine, Yokohama, Japan;* [2]*AIDS Research Center, National Institute of Infectious Diseases, Tokyo, Japan;* [3]*Department of Microbiology, Tokyo Dental College, Chiba, Japan;* [4]*Laboratory of Gene Transfer and Regulation National Institute of Biomedical Innovation, Osaka, Japan;* [5]*Department of Public Health, Yokohama City University, Graduate School of Medicine, Yokohama, Japan; and* [6]*Center for Biologics Evaluation and Research, US Food and Drug Administration, Bethesda, MD, USA*

Immunization involving a DNA vaccine prime followed by an adenovirus type 5 (Ad5) boost elicited a protective immune response against SHIV challenge in monkeys. However, the hepatocellular tropism of Ad5 limits the safety of this viral vector. This study examines the safety and immunogenicity of a replication-defective chimeric Ad5 vector with the Ad35 fiber (Ad5/35) in BALB/c mice and rhesus monkeys. This novel Ad5/35 vector showed minimal hepatotoxicity after intramuscular administration with the novel Ad5/35 vector. In addition, an Ad5/35 vector expressing HIV Env gp160 protein (Ad5/35-HIV) generated strong HIV-specific immune responses in both animal models. Priming with a DNA vaccine followed by Ad5/35-HIV boosting yielded protection against a gp160-expressing vaccinia virus challenge in BALB/c mice. The Ad5/35-HIV vector was significantly less susceptible to the pre-existing Ad5 immunity than a comparable Ad5 vector. These findings indicate that an Ad5/35 vector-based HIV vaccine may be of considerable value for clinical use.
Gene Therapy advance online publication, 4 August 2005; doi:10.1038/sj.gt.3302590

Keywords: *Ad5/35 vector; HIV; animal model; vaccine; immune response*

Introduction

A vaccine capable of preventing HIV infection is needed to control the global AIDS pandemic. In the past decade, multiple strategies to produce an immunogenic HIV vaccine have been explored. This included production of HIV subunit peptide vaccines,[1] DNA vaccines,[2] recombinant virus-vector vaccines (including modified vaccinia virus,[3] adenovirus (Ad),[4,5] rabies virus,[6] flavivirus,[7] sendai virus,[8] Venezuelan equine encephalitis virus,[9] and adeno-associated virus[10,11]), and bacterial vector-vaccines (bacille Calmette–Guerin,[12,13] and *Lactococcus lactis*[14]). Each of these strategies showed some promising results in animal models, either alone or in combination.

Among these vectors, the replication-defective human Ad type 5 (Ad5) recombinants (with the deletion of a replication-essential gene, E1) and the replication-defective modified vaccinia Ankara (MVA) elicited the most potent $CD8^+$ T-cell responses and provided the highest degree of protection in non-human primates.[3,4,15,16] A major limitation for the clinical application of the Ad5 and MVA vectors is the pre-existing immunity against these viruses in humans, since most of the human population has been infected with Ad5[17] and vaccinia virus on being administered the smallpox vaccine. The pre-existing antiviral immunity may strongly influence the efficacy of the HIV vaccine using Ad5 and MVA vectors.

Human Ads are classified into six subgroups from A–F.[18] Most of Ad serotypes belonging to subgroups A, C, D, E, and F use the coxsackievirus and adenovirus receptor (CAR) as a cellular receptor.[19] The Ad5 (subgroup C) has well-defined biological properties and has been widely used as a vector for gene therapy and vaccine. The replication-defective Ad5 vector can easily be produced in high titers and is highly effective in boosting HIV-specific immunity.[4,15] However, this virus uses CAR as its primary attachment receptor, which confers tropism for liver parenchymal cells.[19–22] This raises important safety concerns,[22] particularly because the administration of an Ad5-based vector for gene therapy resulted in the death of a patient.[23] In response to these shortcomings, our laboratory has examined the immunogenicity and safety of a replication-defective chimeric Ad5 vector with Ad type 35 fiber (Ad5/35) (Ad35 virus was classified as subgroup B). The Ad35 fiber showed 25% amino-acid homology with the Ad5 fiber.[24] Cell entry of Ad35 is CAR independent and may involve CD46 receptor, which expresses on most human cells.[25] Ad35 can be transducted to liver nonparenchymal cells on a level 4–5 log orders lower than Ad5, but not to

Correspondence: Dr K Okuda, Department of Molecular Biodefense Research, Yokohama City University, Graduate School of Medicine, 3-9 Fukuura, Kanazawa-ku, Yokohama 236-0004, Japan
Received 3 April 2005; accepted 18 June 2005

liver parenchymal cells.[20] In the present study, we found that the Ad5/35 recombinants not only induced strong antigen-specific humoral and cellular immune responses and exhibited minimal hepatotoxicity in both mice and non-human primates, but were also significantly less susceptible to the pre-existing Ad5 immunity than a comparable Ad5 vector.

Results

Biodistribution of Ad in mice

In the initial experiments, mice were injected intramuscularly (i.m.) with 10^{11} viral particles (vp) of a luciferase-expressing Ad5 (Ad5-Luc) or Ad5/35 vector (Ad5/35-Luc). Luciferase expression was monitored using an *in vivo* imaging system (IVIS) on days 3 and 10 after administration. As shown in Figure 1a, all of the Ad5/35-Luc vector remained at the injection site. In contrast, substantial amounts of the Ad5 vector migrated to the liver. This difference in vector distribution was confirmed by studies involving LacZ-expressing Ad5 and Ad5/35 vectors (data not shown). Studies on serum glutamic-oxaloacetic transaminase (GOT) and serum glutamic-pyruvic transaminase (GPT) levels revealed that mice injected with the Ad5-Luc vector had changes indicative of liver damage (Figure 1b). We also analyzed serum levels of key proinflammatory cytokines (IFN-γ and IL-6) on days 0, 3, and 10 after administration of virus vectors. The levels of IFN-γ and IL-6 were significantly elevated following administration of Ad5-Luc vector, but not of Ad5/35-Luc vector (Figure 1c). Thus, the hepatotoxicity caused by the Ad5 vector was circumvented by the use of an Ad5/35 vector.

Time-course study of HIV-specific immune responses in mice.

Ad5/35 vector can efficiently transfect antigen-presenting cells[18,21,26,27] and muscular cells (Figure 1a). In order to explore whether the virus vector can be used as a vaccine vector, we constructed an HIV Env gp160-expressing Ad5/35 vector (Ad5/35-HIV). The expression of HIV gp160 was confirmed by Western blotting (Figure 2a). The HIV Env gp160-expressing DNA vaccine (DNA-HIV) used in this study was reported previously.[28] The mice were immunized with 10^{10} vp of Ad5/35-HIV vector, and the HIV-specific cellular immune response was periodically monitored by the intracellular cytokine staining (ICS) assay. The assay has been widely utilized to distinguish the relative contributions of $CD8^+$ cells to the overall T-cell responses.[29] On day 3, HIV-specific IFN-γ-secreting $CD8^+$ T cells can be detected (Figure 2b) and peaked 2 weeks after immunization. On day 50 and month 7 after final immunization, 2.5 and 1.2% of HIV-specific IFN-γ-secreting $CD8^+$ T cells still persisted, respectively.

Mice were vaccinated with Ad5/35-HIV vector to explore the humoral immune response 7 weeks after the final immunization. The animals immunized with 10^{10} vp of Ad5/35-HIV vector developed a high-tittered anti-gp160 antibody (Ab) response (Figure 2c). The specificity of the Ab response was confirmed by Western blotting (Figure 2c, upper panel). The magnitude of this response was not significantly altered by preimmunization with the DNA-HIV vaccine (Figure 2c). DNA-HIV vaccination alone generated a low level of HIV-specific serum Ab (Figure 2c, bottom panel). HIV-specific neutralizing Ab was only detectable in the Ad5/35-HIV

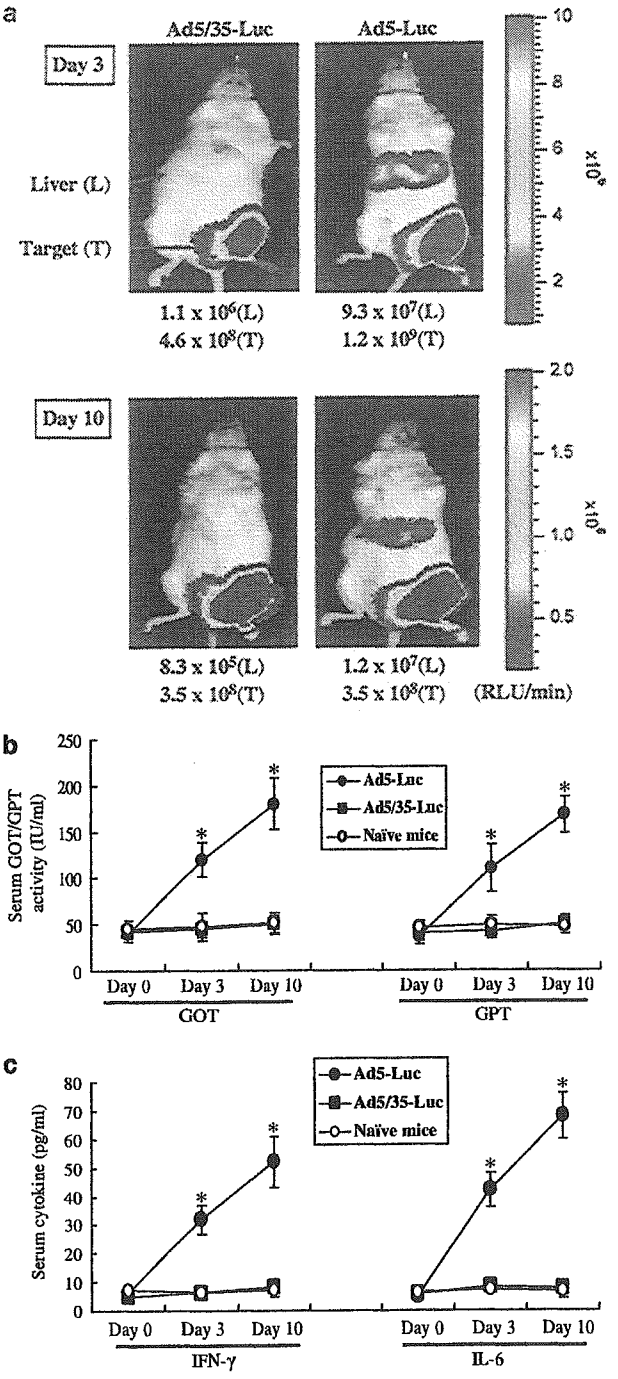

*Figure 1 Biodistribution and safety of Ad vectors. BALB/c mice were injected i.m. with 10^{11} vp of the Ad5-Luc or Ad5/35-Luc vector. (a) Using an IVIS CCD camera, vector distribution was detected after the addition of luciferin (3 mice/group) (expressed in relative light units (RLU)). One of the mice is represented and other mice used show the same pattern. (b) Serum GOP and GPT levels were measured on days 0, 3, and 10 after injection (5 mice/group). IU: international unit. (c) Serum IFN-γ and IL-6 levels were measured on days 0, 3, and 10 after injection (5 mice/group). *Mean values are significantly different between Ad5-Luc-administered mice and Ad5/35-Luc-administered mice or naïve mice at the same time point.*

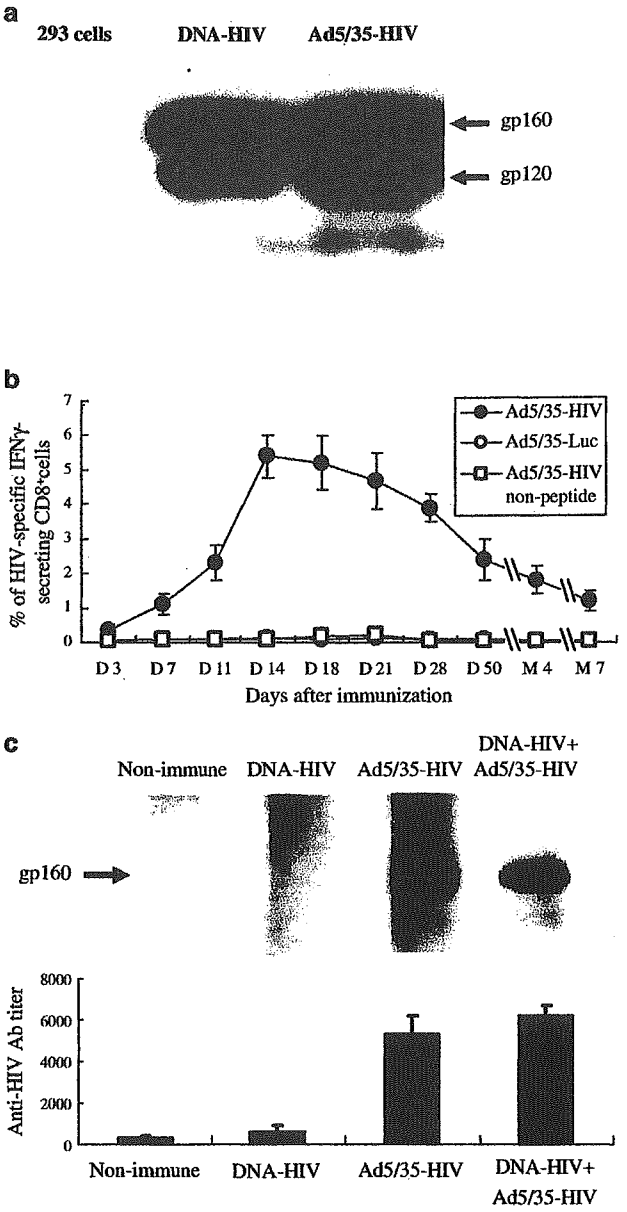

Figure 2 Time course of HIV-specific immune responses in mice. (a) HIV Env protein expression of DNA-HIV vaccine and Ad5/35-HIV on HEK293 cells was confirmed by Western blotting using an HIV Env-specific mAb. (b) Time-course study of cellular immune responses after a single i.m. injection of 10^{10} vp of Ad5/35-HIV vector (3 mice/time point). D: day; M: month. (c) HIV-specific Ab was detected by Western blotting using 100-fold diluted antisera (serum pool of 10 mice/group) (upper panel) and ELISA (10 mice/group) (bottom left panel).

vaccinated mice (1:186) and DNA prime/Ad5/35-HIV boosted mice (1:206).

Immune responses and challenge in mice 2 weeks after vaccination. There is growing evidence that cellular immunity contributes to protecting the host against HIV infection.[3,4,30,31] The ability of the Ad5/35 vector to trigger the activation and proliferation of antigen-specific T cells was monitored. Vaccination with the DNA-HIV vaccine induced the number of HIV-specific IFN-γ-secreting $CD8^+$ T cells to increase from background levels (<0.2–0.7%) ($P<0.05$) (Table 1). This was significantly less than the effect of vaccination with the Ad5/35-HIV vector (10^{10} vp/mouse) that increased the IFN-γ-secreting $CD8^+$ T cells to 5.5% ($P<0.05$). Priming with the DNA-HIV vaccine followed by an Ad5/35-HIV vector boost led to a further three-fold increase in the number of IFN-γ-secreting $CD8^+$ T cells ($P<0.05$).

A tetramer-binding assay was used to verify that the IFN-γ-secreting cells were MHC class I-restricted HIV-specific $CD8^+$ T cells.[32] A single immunization with Ad5/35-HIV vector elicited a significant increase in the number of tetramer-binding $CD8^+$ T cells (Table 1). When compared with DNA-HIV vaccination alone, immunization with the Ad5/35-HIV vector yielded five-fold more HIV-specific $CD8^+$ T cells ($P<0.05$). Priming with the DNA-HIV vaccine, followed by Ad5/35-HIV boosting, further increased the tetramer binding ($P<0.05$).

To examine the protective activity of the Ad5/35-HIV vector, immunized mice were challenged with 10^8 plaque forming units (PFU) of vPE16 2 weeks after final immunization. The animals that were vaccinated with the Ad5/35 vector alone or in combination with the DNA-HIV vaccine were completely protected from infection (Table 1); however, the DNA-HIV vaccination alone had little impact on the susceptibility to infection by vPE16.

Long-term cell-medicated immune responses and challenge in mice. The durability of these vaccine regimens was explored. HIV-specific cellular immune responses persisted through 7 months after final immunization (Table 1 and Figure 2b). To determine whether this immune response was protective, vaccinated mice were challenged with vPE16 (10^8 PFU/mouse) 7 weeks after final immunization. The viral load of Ad5/35-HIV-immunized mice was reduced by 10^5 as compared with that of the control mice ($P<0.05$). DNA-HIV vaccination by itself was not protective, but the combination of DNA-HIV priming and Ad5/35-HIV boosting yielded a prolonged and complete protection (Table 1).

Biodistribution of Ad in rhesus macaques

To study the biodistribution of Ad in monkeys, 10^{11} vp of Ad5-Luc and Ad5/35-Luc vectors was injected i.m. into two rhesus monkeys for each vector. The luciferase activity in the tissues was detected 3 days after administration, because high luciferase activity in the mouse liver was observed at that time point. Liver infection with Ad5 vector was 20- to 40-fold stronger than that with Ad5/35 vector (Figure 3a). It is important to note that the luciferase activity of the cerebellum and the posterior cerebrum in the monkeys that received the Ad5-Luc vector was two- and four-fold higher, respectively, than that of the monkeys that received the Ad5/35-Luc vector.

Immune response in rhesus monkeys after vaccination

To explore the immunogenicity of the Ad5/35-HIV vector in monkeys, two rhesus macaques were immunized i.m. with 10^{11} vp of Ad5/35-HIV vector. A detectable HIV-specific serum Ab response developed

Table 1 HIV-specific cell-mediated immune responses and virus challenge after vaccination

	Week 2			*Week 7*			*Month 4*	*Month 7*
	ICS (%)	*Tetramer (%)*	*Ovary viral titer*	*ICS (%)*	*Tetramer (%)*	*Ovary viral titer*	*Tetramer (%)*	*Tetramer (%)*
Nonimmune	0.1±0.1	0.1±0.1	$8\times10^{8}\pm35$	0.1±0.1	0.1±0.1	$1\times10^{9}\pm65$	0.0±0.0	0.0±0.0
DNA-Empty	0.1±0.1	0.1±0.1	$2\times10^{9}\pm45$	0.0±0.0	0.0±0.0	$8\times10^{8}\pm32$	0.0±0.0	0.0±0.0
Ad5/35-Luc	0.2±0.1	0.2±0.2	$2\times10^{9}\pm25$	0.0±0.0	0.0±0.0	$4\times10^{8}\pm46$	0.0±0.0	0.0±0.0
DNA-HIV	0.7±0.1	1.0±0.3	$6\times10^{6}\pm42$	0.4±0.2	0.6±0.1	$5\times10^{7}\pm51$	0.3±0.1	0.1±0.1
Ad5/35-HIV	5.5±0.3	5.2±0.3	ND	2.5±0.8	3.1±0.2	$2\times10^{3}\pm34$	2.5±0.5	1.2±0.4
DNA-HIV+Ad5/35-HIV	17.2±0.8	19.4±2.1	ND	8.2±1.2	8.9±0.8	ND	7.1±0.6	4.1±0.3

Mice were immunized with DNA plasmid or Ad5/35 vector, either alone or in combination. At 2 weeks, 7 weeks, 4 months, and 7 months after final immunization, HIV-specific cellular immune responses were detected by ICS assay and tetramer assay. The data represent the percentage of IFN-γ- or tetramer-positive $CD8^+$ T cells (5–10 mice/group). The backgrounds were less than 0.1% IFN-γ-secreting $CD8^+$ T cells when cells were stimulated with control peptide (influenza NP peptide, TYQRTRALV). The vaccinated mice (10 mice/group) were challenged with vaccinia virus vPE16 2 or 7 weeks after final immunization. At 6 days after the challenge, the vPE16 titer in mouse ovaries was measured. ND, not detectable.

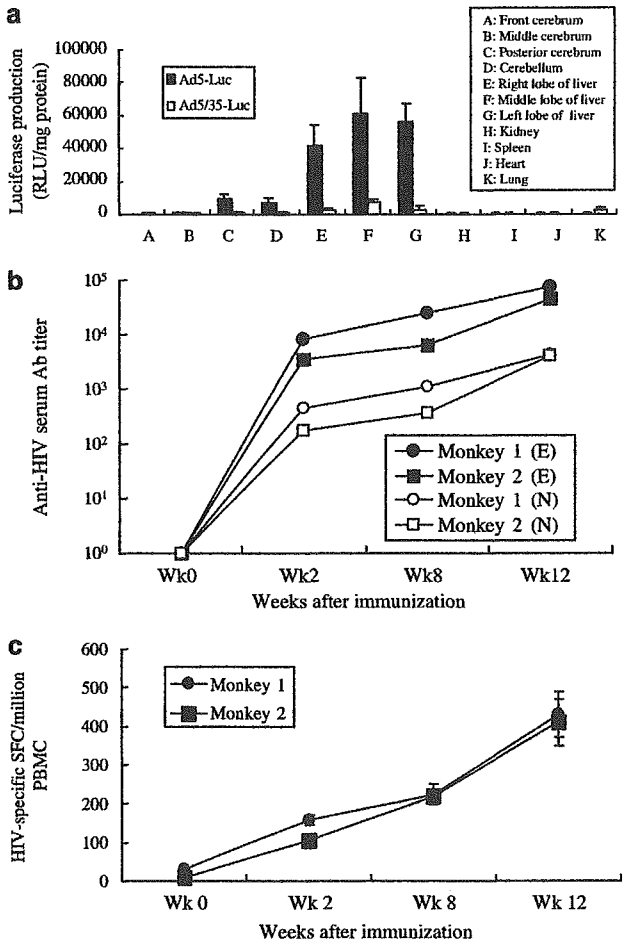

Figure 3 Biodistribution and HIV-specific immune responses in rhesus monkeys. Rhesus monkeys (2 monkeys/group) were administered i.m. 10^{11} vp of Ad5-Luc or Ad5/35-Luc vector. The luciferase activity in the organs of the monkey (expressed in RLU) was examined 3 days after administration (a). Rhesus monkeys were immunized i.m. with 10^{11} vp of Ad5/35-HIV vector at 0 and 8 weeks. PBMCs were isolated at weeks 0, 2, 8, and 12. HIV-specific Ab titers were measured in triplicate by ELISA (E) (●, ■) and neutralizing assay (N) (○, □) (b). The detecting limitation of the neutralizing assay was 100 ND_{50}/ml. PBMCs were stimulated with HIV Env gp120 protein, and the number of cells activated to secrete IFN-γ was determined in triple wells by ELISPOT (c). SFC: spot-forming cells.

within 2 weeks of immunization (Figure 3b). The animals were boosted at 8 weeks. After 4 weeks, titers in excess of 1:50 000 were achieved. Similar results were observed in neutralizing Ab. A increase in the number of HIV-specific IFN-γ-secreting T cells was also detected in the peripheral blood mononuclear cells (PBMCs) (Figure 3c). Boosting with Ad5/35-HIV vector further increased this T-cell response.

Effect of pre-existing immunity on vaccination

To evaluate the effect of the anti-Ad5 neutralization Ab (found in 60% of the adult human population)[17] on the Ad5/35 vector, the infectivity of the vector was examined after incubation with serially diluted serum from subjects with high titers of anti-Ad5 Abs (anti-Ad5 neutralizing titer = 1:64). As shown in Figure 4, the human antisera had 1:8 anti-Ad5/35 neutralizing titer and normal human sera against either Ad5 or Ad5/35 vector was less than 1:4. The sera derived from Ad5/35-HIV-immunized monkeys showed two-fold higher neutralizing Ab titer against Ad5/35 vector than Ad5 vector.

To examine the effect of pre-existing anti-Ad5 immunity on the activity of the Ad5/35 vector *in vivo*, mice were injected i.m. with 10^{10} or 10^{11} vp of Ad5-Luc. After 8 weeks, these animals were immunized with 10^{10} vp of Ad5-HIV or Ad5/35-HIV. The HIV-specific responses were detected by the tetramer assay 2 weeks after immunization. Although pre-existing immunity to Ad5 reduced the immune response elicited by both vectors, Ad5/35-HIV was significantly more immunogenic than Ad5-HIV ($P<0.05$; Figure 4).

Discussion

This study demonstrates that an Ad5/35-HIV vector vaccine induces strong cellular and humoral immune responses with minimal toxicity in mice and rhesus macaques. A prime–boost strategy involving the DNA-HIV vaccine and the Ad5/35-HIV vector generated protective immunity against viral infection in mice.

A widely used HIV vaccine should have high immunogenicity, low cost of production, and low or no pathogenicity. Replication-defective Ad5 is one of the best vectors for HIV vaccine development. Vaccination

with recombinant Ad5 has achieved great success in inducing protection against virus infection in several animal models.[4,15,33] Ad5 is well characterized, and its subclinical disease association in humans is well known.[34,35] However, a majority of the human population (more than 60%) is infected with the Ad5 virus.[17,36,37] The neutralizing Ab and the cellular immune responses against the Ad5 fiber and capsid may reduce the efficacy of the Ad5 vector when it is used in a clinical trial.[37,38] The switching of the Ad serotypes[37,39] and the use of animal Ads[40–44] enables the partial bypass of the pre-existing immune responses to Ad5 viruses. However, there are a few drawbacks: lack of knowledge regarding the biology of these viruses, including tropism on human cells; potential difficulties in manufacturing; and the possibility of *in vivo* recombination with other human viruses leading to unknown diseases. Animal Ad vectors may induce the antigen-specific responses as strongly as Ad5 in animal models.[43] However, their immunogenicity in humans is still unknown. This study used a chimera Ad5 vector with Ad35 fiber, which relates with cell tropism. The Ad5/35, similar to Ad5, has a high productive titer in tissue culture cells, because it is commonly known that human subgroup B Ads, such as Ad5, have a considerably higher titer as compared with other subgroup viruses, including Ad35. Nevertheless, the virus displayed the cell tropism of Ad35. We explored the immunogenicity of the Ad5/35 vector encoding HIV Env gene in both mice and non-human primates. The results indicate that the Ad5/35-HIV vector elicited strong HIV-specific humoral and cellular immune responses that conferred protective immunity (Table 1 and Figure 3b and c). Coupled with the evidence that an Ad5/35 vector transduces human dendritic cells more efficiently as compared with an Ad5 vector,[18,21,26,27] these findings suggest that the Ad5/35-HIV vector is a promising candidate for human trials.

Another concern regarding the use of the Ad5 vector in clinical trials is its strong tropism to hepatocytes that is caused by the high expression of CAR in the hepatocytes. Our experiments showed a high expression of the Ad5 vector in the liver in both mice and non-human primates after i.m. administration, but not of the Ad5/35 vector (Figure 1). In contrast to Ad5 vector, Ad/35 vector did not elevate the levels of serum markers (GOT/GPT) of hepatotoxicity and key proinflammatory cytokines (IFN-γ and IL-6) in mice (Figure 1b and c). These results demonstrate that, as a vaccine vector, Ad5/35 vector is safer than Ad5 vector. However, low expression of Ad5/35 vector in monkey liver was still detected after i.m. administration of Ad5/35-Luc vector to monkeys (Figure 3a). It may have resulted from low capacity of Ad5/35 to infect liver nonparenchymal cells, but not liver parencymal cells.[20] Interestingly, we found a certain magnitude of Ad5 vector expression in the posterior cerebrum and cerebellum of monkeys; however, the Ad5/35 vector was not expressed (Figure 4a). Nevertheless, in the present experiment, we could not precisely define the location of the Ad5-infected cells or determine whether the infection potentially causes local inflammation or toxicity. However, potential brain infection after Ad5 vector administration is a safety concern because intranasal administration of the Ad5 vector has been reported to result in the infection of the central nervous system.[45]

In this study, the effect of pre-existing anti-Ad5 immunity on the Ad5/35 vector was explored along with several immunization protocols as follows. (1) Both *in vitro* and *in vivo* studies demonstrate that the Ad5/35 vector is significantly less susceptible to neutralization by anti-Ad5 Abs as compared with a conventional Ad5 vector (Table 2 and Figure 4). The administration or infection of Ad can induce immune responses against the Ad hexon, penton, and fiber antigens. The exchange of fiber can partially reduce the inhibition of the

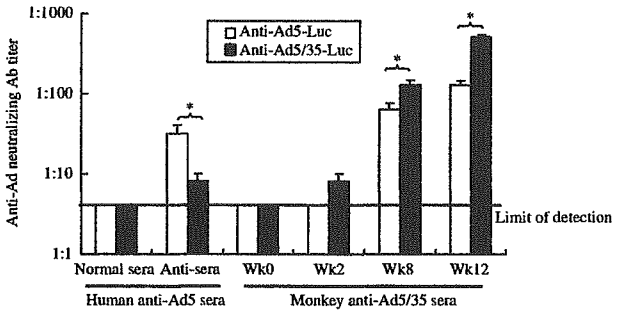

Figure 4 *Effect of pre-existing antiviral immunity. Ad5-Luc and Ad5/35-Luc vectors were incubated with an equal volume of serially diluted normal human sera (No. 2, anti-Ad5 neutralization titer <1:4), human antisera (No. 2, anti-Ad5 neutralization titer = 64), or monkey antisera from Figure 3b and c (No. 2) in triplicate and were subsequently added to infected Vero cells in a 96-well plate at 10^7 vp/well. The luciferase activity was measured 48 h after infection. The neutralizing titer was calculated with limited serum dilution when the luciferase activity in the Ad-infected cells was equal with the background. Average and standard deviations for three independent experiments are shown. *Mean values are significantly different between groups.*

Table 2 Effect of pre-existing antiviral immunity

	Prime	*Anti-Ad5 neutralizing Ab titer*	*Boost*	*Tetramer assay (%)*
Control	Non	<1:4	Ad5-HIV (10^{10} vp/mouse)	4.8±0.2
			Ad5/35-HIV (10^{10} vp/mouse)	5.1±0.2
Low dose	Ad5-Luc (10^{10} vp/mouse)	1:102	Ad5-HIV (10^{10} vp/mouse)	2.3±0.4 *
			Ad5/35-HIV (10^{10} vp/mouse)	4.6±0.6 *
High dose	Ad5-Luc (10^{11} vp/mouse)	1:248	Ad5-HIV (10^{10} vp/mouse)	0.5±0.1 *
			Ad5/35-HIV (10^{10} vp/mouse)	2.6±0.4 *

After 8 weeks, naive mice or mice pretreated with 10^{10} or 10^{11} vp of Ad5-Luc vector (6 mice/group) were immunized with 10^{10} vp of Ad5-HIV or Ad5/35-HIV vector. At the time of vaccination, anti-Ad5 neutralizing titers were measured in Ad5-Luc-treated mice. At 2 weeks after vaccination, the HIV-specific responses were detected by an HIV-specific tetramer assay. *Mean values are significantly different between the groups.

pre-existing immunity against the parent Ads (Table 2 and Figure 4). The exchange of other genes, including hexon and penton, may further reduce the inhibition of pre-existing anti-Ad5 immunity. (2) We also explored the immune responses by using the same vector for prime/boost. When the mice were immunized i.m. with 10^{10} vp of Ad5/35-HIV 1–3 times at 4-week intervals, the HIV-specific cell-mediated immune responses were detected by the tetramer assay. An increased response was observed after the second immunization but not after the third immunization (data not shown). High anti-Ad5/35 neutralizing Ab after second immunization may block the Ad5/35-HIV infection (Figure 4). These results are in agreement with the data from our study on monkeys (Figure 3b and c) and with that from studies by other groups,[33,43] and other virus such as MVA vector may be applicable for further boost if high immune responses are required. The DNA-HIV vaccine prime/Ad5/35-HIV vector boost regimen greatly increased HIV-specific cell-mediated immune responses (Table 1 and Figure 3b and c), but not the humoral immune response (Figure 2c). This suggests that DNA vaccination enhances adenoviral recombinant-induced cell-mediated immunity rather than humoral immunity, as described by other groups.[4,38] Furthermore, DNA vaccine priming can reduce the humoral response to the adenoviral antigens and can counterbalance the impaired B-cell response to the antigen expressed by the adenoviral recombinant in mice that are preimmune to Ad.[46] This DNA prime/Ad5/35 boost regimen might be highly suitable for use in humans with previous exposure to the Ad5 virus. (3) To examine the immunogenicity and protective immunity of the Ad5/35 vector, we used HIV-1 IIIB in this study, because the strain has been well studied and we can compare our data from the new vector with that from other studies. For the clinical trail, we have constructed DNA vaccine and Ad5/5 vector expressing ENV and GAG of a Clade C HIV-1 isolate and similar results with HIV-1 IIIB strain were obtained in a mouse model (manuscript in preparation).

Considered together, using Ad5/35 vector, we developed an HIV vaccine with a higher immunogenicity and low pathogenicity. The Ad5/35-HIV vaccine induced strong HIV-specific immune responses in both BALB/c mice and rhesus monkeys. Priming with a DNA-HIV vaccine followed by Ad5/35-HIV boosting yielded protection against viral infection in mice. The Ad5/35 vector may be a promising vaccine for human clinical trial.

Materials and methods

Recombinant vectors

E1,E3-deletion, replication-defective recombinant viruses were constructed with an Ad generation kit (Avior Therapeutics Inc., Seattle, WA, USA).[21] Briefly, a 5.2k bp *Sal*I/*Pst*I fragment containing CAG promoter-HIV_{IIIB} rev/env gp160-polyA was isolated from pCAGrev/env.[28] A shuttle plasmid (pLHSP) containing Ad5 positions 22–342, Ad5 3523–5790, *Escherichia coli ori*, and ampicillin-resistant gene was obtained from Avior Therapeutics Inc. (Seattle, WA, USA). The 5.2k bp blunted fragment was subcloned into blunted *Eco*RI site of pLHSP plasmid vector to generate pLHSP-HIV shuttle plasmid. The pLHSP-HIV shuttle plasmid was linearized with *Pac*I and transfected with E1,E3-deletion, chimeric Ad5 or 5/35 genome to human embryonic kidney (HEK293) cells using calcium precipitation method to generate recombinant virus, Ad5-HIV and Ad5/35-HIV, respectively. The recombinant virus (Ad5/35-HIV, Ad5-HIV) was propagated in HEK293 cells and purified by two repetitions of the CsCl methods described elsewhere.[47] The total concentration of virions in each preparation was calculated from the optical density at 260 nm (OD_{260}), using the formula 1 $OD_{260} = 1 \times 10^{12}$ vp/ml. The HIV_{BH8} gp160-expressing replication-competent vaccinia virus (WR strain, vPE16; HIV_{BH8} gp160 has 97.32% amino-acid homology with HIV_{IIIB} gp160) was obtained from the AIDS Research and Reagent Program, National Institutes of Health, Rockville, MD, USA (Cat. No. 362). The vPE16 vectors were propagated in CV1 cells. The Ad5-Luc and Ad5/35-Luc vectors expressing luciferase coding gene were described previously.[26] The DNA-HIV vaccine (pCAGrev/env) containing HIV_{IIIB} *rev* and *env* genes has been previously reported.[28]

Biodistribution of Ad5 and Ad5/35 vectors in vivo

The experiment was performed as previously described.[48,49] In brief, the Ad5-Luc or Ad5/35-Luc vectors (10^{11} vp/mouse) were injected i.m. into BALB/c mice. On days 3 and 10, the mice were anesthetized with a 2% isofluorane/air mixture, and a single dose of 150 mg/kg luciferin in normal saline was administered intraperitoneally. The CCD images were obtained using a cooled *in vivo* imaging system (IVIS) CCD camera (Xenogen, Alameda, CA, USA) and analyzed. To study the viral biodistribution in primates, two rhesus monkeys (2 years old, male) were administered i.m. 10^{11} vp of Ad5-Luc or Ad5/35-Luc. At 3 days after administration, the luciferase activity was detected in the monkey organs (brain, liver, kidney, spleen, heart, and lung) using the Luciferase Assay Systems (Promega, Madison, WI, USA). Serum GOT and serum GPT were measured in mouse or monkey sera at the Kitayama-Rabesu Institute (Ina, Nagano, Japan). The concentration of serum IFN-γ and IL-6 was measured using the IFN-γ and IL-6 ELISA kits (Biosource, Camarillo, CA, USA), respectively, according to the manufacturer's protocol.

Animal immunization

Female BALB/c mice (8-week-old; H-$2D^d$) were purchased from Japan SLC Inc., Shizuoka, Shizuoka-ken, Japan. The mice were immunized with an i.m. injection of 100 μg of pCAGrev/env or pCAGempty plasmid DNA in phosphate-buffered saline (PBS) at 0, 1, and 2 weeks and were boosted with 10^{10} vp of Ad5/35-HIV or Ad5/35-Luc vector at week 3. For the time-course study, the mice were administered a single i.m. injection of 10^{10} vp of Ad5/35-HIV vector per mouse. To study the effect of pre-existing antiviral immunity on vaccination, the mice were injected i.m. with 10^{10} or 10^{11} vp of Ad5-Luc vector and then immunized 8 weeks later with 10^{10} vp of Ad5-HIV vector or Ad5/35-HIV vector. For rhesus monkey immunization, 10^{11} vp of Ad5/35-HIV vector was injected i.m. into two rhesus monkeys (2 years old, male) at weeks 0 and 8.

Intracellular cytokine staining assay

IFN-γ-secreting $CD8^+$ T cells were detected by the protocol recommended by the manufacturer (Cytofix/CytoPerm Plus kit, PharMingen, San Diego, CA, USA). In brief, lymphocytes were isolated from the mouse spleen. A single cell suspension was incubated with 10 μg/ml of the HIV V3 peptide (NNTRKRIQRGP GRAFVTIGKIGN) for 24 h at 37°C. At 2 h before the end of incubation, 1 μg/ml of GolgiPlug was added. The cells were washed with staining buffer (3% fetal calf serum (FCS), 0.1% sodium azide (NaN_3) in PBS), blocked with 4% normal mouse sera, and stained with phycoerythrin (PE)-conjugated anti-mouse CD8 Ab (Ly-2, PharMingen). The cells were then suspended in 250 μl of Cytofix/Cytoperm solution at 4°C for 20 min, washed with Perm/Wash solution, and stained with anti-mouse IFN-γ Ab conjugated with fluorescein isothiocyanate (FITC) (PharMingen) at 4°C for 30 min, followed by flow cytometric analysis.

Tetramer assay

The tetramer assay used a PE-conjugated H-$2D^d$/p18 tetramer (RGPGRAFVTI), as previously described.[28] In brief, splenocytes were isolated from mice and incubated for 30 min at 4°C with 4% normal mouse serum in PBS. Cells were stained with FITC-conjugated anti-mouse CD8 Ab (Ly-2, PharMingen) for 30 min at 4°C. After washing twice with the staining buffer (3% FCS, 0.1% NaN_3 in PBS), the cells were incubated with the tetramer reagent for 15 min at 37°C, followed by flow cytometric analysis (Becton Dickinson).

Recombinant vaccinia virus used for the challenge study

Using vPE16 vaccinia virus, the virus challenge experiment was performed as described previously.[28] Vaccinated female mice were intraperitoneally challenged with 10^8 PFU of vaccinia virus vPE16 at 2 or 7 weeks after the final immunization. At 6 days after challenge, the mice were killed, their ovaries were sonicated, and the vPE16 titer was determined by serial 10-fold dilution on a plate of CV1 cells. Infected cells were detected by staining with crystal violet and plaques were counted at each dilution.

Detection of HIV-1-specific Ab

The HIV-1-specific Ab was detected by the Western blotting method and the enzyme-linked immunosorbent assay (ELISA). By Western blotting method, the HIV envelope glycoprotein gp160-coated membrane from the New Lav Blot 1 kit (Bio-Rad, Marnes-la-Coquette, France) was incubated with a 100-fold dilution of mouse serum followed by an affinity-purified horseradish peroxidase (HRP)-labeled anti-mouse immunoglobulin (ICN Pharmaceuticals Inc., OH, USA). HIV gp160 protein was detected using the ECL Plus Western Blotting Detection System (Amersham Pharmacia Biotech).

ELISA was performed as described elsewhere.[10] To summarize, 96-well microtiter plates were coated with 10 μg/ml of HIV_{IIIB} gp120 protein (donated by AIDS Research and Reference Reagent Program, National Institutes of Health) and incubated overnight at 4°C. The wells were blocked with PBS containing 1% bovine serum albumin (BSA) for 2 h at room temperature. They were then treated with 100 μl of serially diluted antisera and incubated for an additional 2 h at 37°C. The bound immunoglobulin was quantified using an affinity-purified HRP-labeled anti-mouse Ab or anti-monkey Ab (both from Sigma). The mean Ab titer was expressed as the reciprocal of the serial serum dilution that exceeded the assay background by 2 s.d.

The HIV-specific neutralizing titer of immune mice or monkeys was also measured. The serially diluted antisera were incubated with 200–300 blue spot-forming units (BFU) of $HIV\text{-}1_{LAI}$ at 37°C for 1 h. The mixture was incubated with confluent MAGIC5 cells (from Dr Tatsumi, National Institute of Infectious Diseases, Tokyo, Japan),[50,51] Dulbecco's modified Eagle's medium (DMEM) with 10% FCS and 0.2 mg/ml of G418 in a 96-well plate at 37°C for 2 days. The cells were fixed with fixing solution (1% formaldehyde, 0.2% glutaraldehyde in PBS) for 5 min and stained with staining solution (4 mM potassium ferrocyanide, 4 mM potassium ferricyanide, 2 mM magnesium chloride, 0.4 mg/ml X-gal in PBS) at 37°C for 18–24 h. The staining was stopped by removing the staining solution and the cells were washed twice with PBS. The blue spot in each well was counted after the staining, and the neutralizing titer was calculated as (1−(% infection/% infection of control wells)) × 100. The 50% neutralization dose (ND_{50}) is defined as the concentration of the Ab that reduced the number of infected cells by 50%. The detecting limitation of the assay was 100 ND_{50}/ml.

ELISPOT assay

The frequency of HIV-specific IFN-γ-secreting cells in monkeys was determined using an ELISPOT assay kit (U-Cytech, Utrech, The Netherlands) according to the manufacturer's manual. In brief, 2×10^5 monkey PBMCs were stimulated in triplicate wells with 1 μg/ml of the HIV_{IIIB} gp120 protein for 16 h at 37°C. Nonstimulated cells were used to assess the background. The cells were transferred to an anti-IFN-γ Ab-coated 96-well plate and incubated for 5 h at 37°C. The cells were removed and 200 μl/well of ice-cold deionized water was added to lyse the remaining PBMCs. Subsequently, the plate was washed with PBS containing 0.05% Tween 20 (PBS-T) and incubated with biotinylated anti-IFN-γ Ab for 1 h at 37°C. After 10 washings with PBS-T, 50 μl of gold-labeled anti-biotin Ab was added and incubated for 1 h at 37°C. The plate was washed 10 times with PBS-T, and 30 ml of activator solutions was added. The plate was incubated in the dark for 30 min at room temperature to develop spot formations. After 30 min incubation, the plate was washed with deionized water and air-dried; spots were counted by a computer-assisted video image analysis. The results were expressed as spot-forming cells (SFC) per million cells.

Ad-specific neutralizing assay

Ad5-Luc or Ad5/35-Luc vector (10^7 vp) was incubated with an equal volume of serially diluted normal human sera (anti-Ad5 neutralizing titer <1:4), human antisera (anti-Ad5 neutralizing titer = 1:64), or monkey sera (at weeks 0, 2, 8, and 12 after immunization with Ad5/35-HIV vector) at 37°C for 2 h. The mixture was incubated with confluent Vero cells in a 96-well plate at 37°C for an additional 48 h. The luciferase activity was detected by Luciferase Assay Systems (Promega, Madison, WI, USA).

The neutralizing titer was calculated with limited serum dilution when the luciferase activity in the Ad-infected cells was equal with the background.

Data analysis

All values were expressed as means ± standard error (s.e.). Statistical analysis of the experimental data and controls was conducted with one-way factorial analysis of variance. Significance was defined at $P<0.05$ in the statistical analysis.

Acknowledgements

We are grateful to M Kawano, T Takeishi, and T Matsuda for their technical assistance and A De La Fuente for her secretarial assistance. This work was partially supported by a Grant-in-Aid from the Ministry of Education, Science, Sports, and Culture of Japan, and the grant for 2005 Strategic Research Project (No. K17018) of Yokohama City University, Japan.

References

1 Bukawa H *et al.* Neutralization of HIV-1 by secretory IgA induced by oral immunization with a new macromolecular multicomponent peptide vaccine candidate. *Nat Med* 1995; **1**: 681–685.
2 Barouch DH *et al.* Control of viremia and prevention of clinical AIDS in rhesus monkeys by cytokine-augmented DNA vaccination. *Science* 2000; **290**: 486–492.
3 Robinson HL *et al.* Neutralizing antibody-independent containment of immunodeficiency virus challenges by DNA priming and recombinant pox virus booster immunizations. *Nat Med* 1999; **5**: 526–534.
4 Shiver JW *et al.* Replication-incompetent adenoviral vaccine vector elicits effective anti-immunodeficiency-virus immunity. *Nature* 2002; **415**: 331–335.
5 Patterson LJ *et al.* Protection against mucosal simian immunodeficiency virus SIV(mac251) challenge by using replicating adenovirus-SIV multigene vaccine priming and subunit boosting. *J Virol* 2004; **78**: 2212–2221.
6 Schnell MJ *et al.* Recombinant rabies virus as potential live-viral vaccines for HIV-1. *Proc Natl Acad Sci USA* 2000; **97**: 3544–3549.
7 Mandl CW *et al. In vitro*-synthesized infectious RNA as an attenuated live vaccine in a flavivirus model. *Nat Med* 1998; **4**: 1438–1440.
8 Matano T *et al.* Cytotoxic T lymphocyte-based control of simian immunodeficiency virus replication in a preclinical AIDS vaccine trial. *J Exp Med* 2004; **199**: 1709–1718.
9 Caley IJ *et al.* Venezuelan equine encephalitis virus vectors expressing HIV-1 proteins: vector design strategies for improved vaccine efficacy. *Vaccine* 1999; **17**: 3124–3135.
10 Xin KQ *et al.* Oral administration of recombinant adeno-associated virus elicits human immunodeficiency virus-specific immune responses. *Hum Gene Ther* 2002; **13**: 1571–1581.
11 Xin KQ *et al.* A novel recombinant adeno-associated virus vaccine induces a long-term humoral immune response to human immunodeficiency virus. *Hum Gene Ther* 2001; **12**: 1047–1061.
12 Aldovini A, Young RA. Humoral and cell-mediated immune responses to live recombinant BCG-HIV vaccines. *Nature* 1991; **351**: 479–482.
13 Someya K *et al.* Vaccination of rhesus macaques with recombinant *Mycobacterium bovis* bacillus Calmette–Guerin Env V3 elicits neutralizing antibody-mediated protection against simian-human immunodeficiency virus with a homologous but not a heterologous V3 motif. *J Virol* 2005; **79**: 1452–1462.
14 Xin KQ *et al.* Immunogenicity and protective efficacy of orally administered recombinant *Lactococcus lactis* expressing surface-bound HIV Env. *Blood* 2003; **102**: 223–228.
15 Sullivan NJ *et al.* Development of a preventive vaccine for Ebola virus infection in primates. *Nature* 2000; **408**: 605–609.
16 Amara RR *et al.* Different patterns of immune responses but similar control of a simian-human immunodeficiency virus 89.6P mucosal challenge by modified vaccinia virus Ankara (MVA) and DNA/MVA vaccines. *J Virol* 2002; **76**: 7625–7631.
17 Vogels R *et al.* Replication-deficient human adenovirus type 35 vectors for gene transfer and vaccination: efficient human cell infection and bypass of preexisting adenovirus immunity. *J Virol* 2003; **77**: 8263–8271.
18 Havenga MJ *et al.* Exploiting the natural diversity in adenovirus tropism for therapy and prevention of disease. *J Virol* 2002; **76**: 4612–4620.
19 Roelvink PW *et al.* The coxsackievirus-adenovirus receptor protein can function as a cellular attachment protein for adenovirus serotypes from subgroups A, C, D, E, and F. *J Virol* 1998; **72**: 7909–7915.
20 Sakurai F, Mizuguchi H, Yamaguchi T, Hayakawa T. Characterization of *in vitro* and *in vivo* gene transfer properties of adenovirus serotype 35 vector. *Mol Ther* 2003; **8**: 813–821.
21 Shayakhmetov DM, Papayannopoulou T, Stamatoyannopoulos G, Lieber A. Efficient gene transfer into human CD34(+) cells by a retargeted adenovirus vector. *J Virol* 2000; **74**: 2567–2583.
22 Adams JY *et al.* Visualization of advanced human prostate cancer lesions in living mice by a targeted gene transfer vector and optical imaging. *Nat Med* 2002; **8**: 891–897.
23 Thomas CE, Ehrhardt A, Kay MA. Progress and problems with the use of viral vectors for gene therapy. *Nat Rev Genet* 2003; **4**: 346–358.
24 Gao W, Robbins PD, Gambotto A. Human adenovirus type 35: nucleotide sequence and vector development. *Gene Therapy* 2003; **10**: 1941–1949.
25 Gaggar A, Shayakhmetov DM, Lieber A. CD46 is a cellular receptor for group B adenoviruses. *Nat Med* 2003; **9**: 1408–1412.
26 Mizuguchi H, Hayakawa T. Adenovirus vectors containing chimeric type 5 and type 35 fiber proteins exhibit altered and expanded tropism and increase the size limit of foreign genes. *Gene* 2002; **285**: 69–77.
27 Seshidhar Reddy P *et al.* Development of adenovirus serotype 35 as a gene transfer vector. *Virology* 2003; **311**: 384–393.
28 Jounai N *et al.* Contribution of the *rev* gene to the immunogenicity of DNA vaccines targeting the envelope glycoprotein of HIV. *J Gene Med* 2003; **5**: 609–617.
29 Maino VC, Picker LJ. Identification of functional subsets by flow cytometry: intracellular detection of cytokine expression. *Cytometry* 1998; **34**: 207–215.
30 Letvin NL *et al.* Heterologous envelope immunogens contribute to AIDS vaccine protection in rhesus monkeys. *J Virol* 2004; **78**: 7490–7497.
31 Barouch DH *et al.* Reduction of simian-human immunodeficiency virus 89.6P viremia in rhesus monkeys by recombinant modified vaccinia virus Ankara vaccination. *J Virol* 2001; **75**: 5151–5158.
32 Altman JD *et al.* Phenotypic analysis of antigen-specific T lymphocytes. *Science* 1996; **274**: 94–96.
33 Sullivan NJ *et al.* Accelerated vaccination for Ebola virus haemorrhagic fever in non-human primates. *Nature* 2003; **424**: 681–684.
34 Wadell G. Molecular epidemiology of human adenoviruses. *Curr Top Microbiol Immunol* 1984; **110**: 191–220.
35 De Jong JC *et al.* Adenoviruses from human immunodeficiency virus-infected individuals, including two strains that represent new candidate serotypes Ad50 and Ad51 of species B1 and D, respectively. *J Clin Microbiol* 1999; **37**: 3940–3945.

36 Kostense S *et al.* Adenovirus types 5 and 35 seroprevalence in AIDS risk groups supports type 35 as a vaccine vector. *Aids* 2004; **18**: 1213–1216.
37 Barouch DH *et al.* Immunogenicity of recombinant adenovirus serotype 35 vaccine in the presence of pre-existing anti-Ad5 immunity. *J Immunol* 2004; **172**: 6290–6297.
38 Casimiro DR *et al.* Comparative immunogenicity in rhesus monkeys of DNA plasmid, recombinant vaccinia virus, and replication-defective adenovirus vectors expressing a human immunodeficiency virus type 1 *gag* gene. *J Virol* 2003; **77**: 6305–6313.
39 Morral N *et al.* Administration of helper-dependent adenoviral vectors and sequential delivery of different vector serotype for long-term liver-directed gene transfer in baboons. *Proc Natl Acad Sci USA* 1999; **96**: 12816–12821.
40 Hofmann C *et al.* Ovine adenovirus vectors overcome preexisting humoral immunity against human adenoviruses *in vivo*. *J Virol* 1999; **73**: 6930–6936.
41 Farina SF *et al.* Replication-defective vector based on a chimpanzee adenovirus. *J Virol* 2001; **75**: 11603–11613.
42 Moffatt S, Hays J, HogenEsch H, Mittal SK. Circumvention of vector-specific neutralizing antibody response by alternating use of human and non-human adenoviruses: implications in gene therapy. *Virology* 2000; **272**: 159–167.
43 Pinto AR *et al.* Induction of CD8+ T cells to an HIV-1 antigen through a prime boost regimen with heterologous E1-deleted adenoviral vaccine carriers. *J Immunol* 2003; **171**: 6774–6779.
44 Fitzgerald JC *et al.* A simian replication-defective adenoviral recombinant vaccine to HIV-1 *gag*. *J Immunol* 2003; **170**: 1416–1422.
45 Lemiale F *et al.* Enhanced mucosal immunoglobulin A response of intranasal adenoviral vector human immunodeficiency virus vaccine and localization in the central nervous system. *J Virol* 2003; **77**: 10078–10087.
46 Xiang ZQ, Pasquini S, Ertl HC. Induction of genital immunity by DNA priming and intranasal booster immunization with a replication-defective adenoviral recombinant. *J Immunol* 1999; **162**: 6716–6723.
47 Lieber A, He CY, Kirillova I, Kay MA. Recombinant adenoviruses with large deletions generated by Cre-mediated excision exhibit different biological properties compared with first-generation vectors *in vitro* and *in vivo*. *J Virol* 1996; **70**: 8944–8960.
48 Bhaumik S, Gambhir SS. Optical imaging of *Renilla* luciferase reporter gene expression in living mice. *Proc Natl Acad Sci USA* 2002; **99**: 377–382.
49 Lipshutz GS *et al.* *In utero* delivery of adeno-associated viral vectors: intraperitoneal gene transfer produces long-term expression. *Mol Ther* 2001; **3**: 284–292.
50 Mochizuki N *et al.* An infectious DNA clone of HIV type 1 subtype C. *AIDS Res Hum Retroviruses* 1999; **15**: 1321–1324.
51 Mukai T *et al.* Construction and characterization of an infectious molecular clone derived from the CRF01_AE primary isolate of HIV type 1. *AIDS Res Hum Retroviruses* 2002; **18**: 585–589.

International Immunology, Vol. 17, No. 5, pp. 513–522
doi:10.1093/intimm/dxh231

Anti-CD3 induces bi-phasic apoptosis in murine intestinal epithelial cells: possible involvement of the Fas/Fas ligand system in different T cell compartments

Naoko Miura[1], Masahiro Yamamoto[1], Masato Fukutake[1], Nobuhiro Ohtake[1], Seiichi Iizuka[1], Atsushi Ishige[1], Hiroshi Sasaki[1], Kazunori Fukuda[2], Tatsuo Yamamoto[3] and **Satoshi Hayakawa[3]**

[1]Tsumura Research Institute, Tsumura & Co., 3586 Yoshiwara, Ami-machi, Inashiki-gun, Ibaraki 300-1192, Japan
[2]Department of Oriental Medicine, Gifu University School of Medicine, Gifu, Japan
[3]Department of Obstetrics and Gynaecology, Nihon University School of Medicine, Tokyo, Japan

Keywords: crypt, intestinal injury, intestinal intraepithelial lymphocytes, splenocytes, villus

Abstract

Recent studies have suggested that Fas-mediated apoptosis is involved in the pathogenesis of intestinal injury. In this study, we determined the role of Fas/Fas ligand (FasL) interactions in different T cell compartments using a murine model of small intestinal injury. An intraperitoneal injection of 145-2C11 (anti-CD3) antibody into C3H/HeN, BALB/c and MRL mice induced mucosal flattening and rapid, bi-phasic intestinal epithelial cell (IEC) apoptosis, which was detected by conventional light and electron microscopy and by terminal deoxynucleotidyl transferase-mediated dUTP nick-end labeling. In the first, early phase, villous apoptosis was observed up to 4 h after injection, and in the second, later phase, apoptotic crypt cells gradually accumulated for up to 24 h. The early and later phases of apoptosis were reduced in *lpr/lpr* and nude mice compared with those in control strains. In addition, the kinetics of Fas-mediated killer activity induced by the antibody injection were different between intestinal intraepithelial lymphocytes (IEL) and splenocytes (SPL) and seemed to correlate with the bi-phasic occurrence of the apoptosis. Finally, the transfer of intestinal IEL from euthymic to nude mice induced both phases of apoptosis, whereas SPL induced the second phase's crypt apoptosis only by the antibody injection. Together, these results suggest the involvement of Fas-mediated killer activity of thymus-derived T cells in different compartments. Namely, T cell populations in different compartments are differentially involved in the induction of IEC apoptosis and contribute to the complex pathogenesis of immune-mediated intestinal injury in which Fas/FasL interactions may play a critical role.

Introduction

A consensus is emerging that T cells play a central role in the development of intestinal inflammation. Activated T cells are involved in both regulatory and effector mechanisms in inflammatory responses. The effector mechanisms are important for defense against enterobacteria, but may also cause significant bystander tissue damage such as villous atrophy, which may be due to increased intestinal epithelial cell (IEC) apoptosis. Indeed, abnormal T cell activation has been reported in some enteropathies, such as Crohn's disease, ulcerative colitis and celiac disease (1–3).

Activated T cells mediate cytotoxicity through several mechanisms, of which, the Fas/Fas ligand (FasL) system plays an important role. Recent studies have demonstrated that the FasL molecule is expressed on either systemic and/or mucosal lymphocytes in enteropathies such as ulcerative colitis (4, 5) and celiac disease (6–10). In animal models of intestinal injury, several studies have shown that Fas/FasL-mediated cytotoxicity by mucosal lymphocytes may be partly responsible for the enteropathy (11–15). The type and function of the immune components involved in intestinal damage are,

Correspondence to: N. Miura; E-mail: miura_naoko@mail.tsumura.co.jp

Transmitting editor: H. Kikutani

Received 8 April 2003, *accepted* 3 February 2005

Advance Access publication 18 March 2005

however, still obscure, partly because many players including the immune components are involved in the intestinal immune system. The gut-associated lymphoid tissue comprises four compartments: intestinal epithelium, lamina propria, Peyer's patches and mesenteric lymph nodes (16). Gut tissue is an intersection of the mucosal and systemic immune systems, and interactions between different types of T cells may be critical for the integrity of the intestinal immune system. In the inflammatory state, the infiltration of peripheral leukocytes into the tissue makes the situation far more complicated.

The purpose of this study was to investigate the possible involvement of different T cell compartments in killing IEC *in vivo* using a model of small intestinal injury. T cell activation was evoked systemically by the intraperitoneal administration of anti-CD3 antibody. A direct administration was performed in order to avoid any possible interactions between the stimulator and intestinal contents (food, digestive enzymes and bacterial flora). Then we assessed the involvement of Fas using *in vivo* antibody injection to Fas-deficient mice and *ex vivo* measurements of Fas-mediated killer activity after antibody injection. Further, we determined whether thymus-derived T cells were involved in the observed intestinal injury using nude mice. Finally, we investigated the role of intraepithelial lymphocytes (IEL) and splenocytes (SPL) using cell transfer experiments.

Methods

Animals and mAbs

Male C3H/HeN, MRL-+/+, MRL-*lpr/lpr* (Japan SLC Inc., Shizuoka, Japan), BALB/c and BALB/c *nu/nu* (Japan Charles River Laboratory, Yokohama, Japan) mice bred and maintained under specific pathogen-free conditions were used at 9–10 weeks of age. This study conformed to our institution's guidelines for the care and use of laboratory animals in research. Hamster anti-murine CD3 mAb (145-2C11) and control hamster IgG1κ were obtained from BD Biosciences (San Jose, CA, USA). For flow cytometry, we used FITC-conjugated antibodies against CD3 (145-2C11), CD69 (H1.2F3), Fas (Jo2), control hamster IgG1κ, IgG1λ, IgG2λ, PE-conjugated FasL (MFL3) and control hamster IgG1κ (BD Biosciences).

Histology

Mice that received a single intraperitoneal injection of titrated concentrations of anti-CD3 antibody diluted in 100 μl of saline were sacrificed at different time points. The small intestines were removed, fixed and embedded in paraffin according to routine procedures. We quantified apoptotic cells by the method used in the previous studies of the intestinal injury model with minor modifications (17–20). In brief, we have counted damaged cells that have condensing or fragmenting nuclei, classical and definitive features of apoptosis, by light microscopic observation of hematoxylin and eosin (H&E)-stained histological sections. Apoptotic cells in 21 pairs of an adjacent villus and crypt (hereafter the pair will be expressed as a 'villus per crypt unit') were counted in seven random high fields (×400 magnification) per mice. Data represent the number of apoptotic cells in a villus or crypt per unit separately. This classical method of detecting apoptosis is incomplete in terms of the determination of absolute number of apoptosis because of the presence of fragmented cell debris and the very early stage-apoptotic cells in which the changes in nuclei have not occurred yet, however, it can assess the degree of apoptosis at least enough to demonstrate the time- and site-dependent changes of apoptotic changes in small intestines. The terminal deoxynucleotidyl transferase-mediated dUTP nick-end labeling (TUNEL) assay (*In situ* apoptosis detection kit, Intergen Company, NY, USA) was used for only qualitative detection of DNA fragmentation because the TUNEL assay, when used to quantify IEC apoptosis, has been reported to give conflicting results (21). For electron microscopy, samples of small intestine were fixed in 2% glutaraldehyde and processed using routine methods.

Fas-mediated cytotoxicity assay

We analyzed the Fas-mediated cytotoxicity of lymphocytes obtained from mice after anti-CD3 injection. IEL, SPL, mesenteric lymph node cells (MLNC) and Peyer's patch lymphocytes (PPL) were prepared by the method of Taguchi *et al.* (22). The Fas-positive human cell line, Jurkat, was obtained from the American Type Culture Collection (Rockville, MD, USA). Fas-mediated cytotoxicity was assessed according to the method of Lin *et al.* (23), with modifications. This assay is based on the fact that both murine and human FasL can kill Jurkat cells equally well and that the observed cytotoxicity is exclusively dependent on Fas (24). Briefly, [^{3}H]thymidine-labeled Jurkat cells (2×10^4 per well) were cultured with freshly isolated lymphocytes at different Effecter/Target (E/T) ratios in flat-bottomed 96-well plates, previously coated or not coated with 7.4 μg ml^{-1} of anti-CD3 antibody. After cultivation, the cells were lysed and harvested onto two-layered filters: a diethylaminoethyl (DEAE) glass filter to trap fragmented DNA and an unmodified glass filter to trap intact chromatin (25). The percentage of DNA fragmentation was calculated as follows:

$$\%\,\text{DNA fragmentation} = \{\text{c.p.m. DEAE filter}/(\text{c.p.m. glass filter} + \text{c.p.m. DEAE filter})\} \times 100.$$

The expression of cell surface markers was analyzed by flow cytometry (FACScan, BD Biosciences), and data were processed using the Macintosh CELLQuest program (BD Biosciences).

Adoptive transfer of immune cells

Experiment 1. Freshly isolated SPL (5×10^7) or IEL (1×10^7) from 9- to 10-week-old BALB/c mice were transferred intravenously into BALB/c *nu/nu* mice. The following day, anti-CD3 antibody was injected intraperitoneally. Small intestines were removed at 4 and 24 h after the injection and prepared for histological analysis. In the dual-grafting experiment, donor SPL (5×10^7) and IEL (1×10^7) were successively engrafted into BALB/c *nu/nu* mice.

Experiment 2. Freshly isolated IEL (1×10^7) from 6- to 11-week-old BALB/c mice were transferred intravenously into BALB/c *nu/nu* mice. After 5 weeks, anti-CD3 antibody was injected intraperitoneally. In the dual-grafting experiment,

donor SPL (5×10^7) were engrafted at 24 h before the anti-CD3 antibody injection.

Statistical analysis

Statistical comparisons were made using Scheffe's method after analysis of variance. The results were considered significantly different when $P < 0.05$. All analyses were carried out using StatView version 5.0 (SAS Institute Inc., Cary, NC, USA).

Results

Anti-CD3 antibody injection induces bi-phasic apoptosis in IEC

Anti-CD3 antibody induced apoptosis in many IEC in the small intestinal villus and crypts in a bi-phasic manner (i.e. early and late) (Figs 1–3). In the first phase, apoptosis of ciliated villous IEC with condensed nuclei (Figs 2B, D, G and 3A) began to appear at 2 h after the injection, peaked at 4 h and declined thereafter (Fig. 1A). The intestine showed villous shortening and a decline in the number of IEC (Fig. 2C). In the second phase, apoptosis of crypt IEC (Figs 2C, E, H and 3B) increased gradually for 24 h. In addition to H&E staining, TUNEL staining (Fig. 2G and H) and electron microscopic findings (Fig. 3) at 4 and 24 h clearly showed that both phases of apoptosis were induced mainly in IEC, although TUNEL-positive cells were also observed in the lamina propria from 2 to 24 h. Apoptotic bodies in the villus and the crypt decreased to normal levels by days 3 and 4, respectively (data not shown). A low level of crypt hyperplasia and villous atrophy was observed at 4 h and markedly from 24 to 48 h. Inflammatory infiltrates of mononuclear cells were noted in the lamina propria at day 2, but the histological features returned almost to normal by day 4 (data not shown). Apoptotic bodies increased dose dependently, reaching a plateau at a dose of 12.5 μg per mouse in the villus at 4 h and 6.3 μg per mouse in the crypt at 24 h (Fig. 1B and C). Therefore, all further experiments were performed using a dose of 12.5 μg CD3 antibody per mouse. The administration of control hamster IgG1κ had no effect on IEC apoptosis levels or histology (data not shown).

Apoptosis in IEC is induced by anti-CD3 via Fas/FasL interactions in vivo

IEC constitutively express Fas (11, 26), and IEL exert potent Fas-mediated killing activity after *in vitro* CD3 stimulation (27). To investigate whether Fas is involved in the apoptosis observed here, we used the Fas-deficient strain, MRL-*lpr/lpr* (Fig. 4). In MRL-+/+, normal Fas-expressing mice, bi-phasic apoptosis was induced by anti-CD3 injection to the same level as observed in C3H/HeN. On the other hand, in MRL-*lpr/lpr*, apoptosis in both phases was markedly reduced. These results suggest that the Fas/FasL system mediates a large portion of the observed apoptosis.

The *in vivo* administration of anti-CD3 may result in the stimulation of different types of T lymphocytes. Therefore, to clarify which T cell compartments, IEL, PPL, MLNC and SPL, were activated and presented cytotoxicity by the anti-CD3

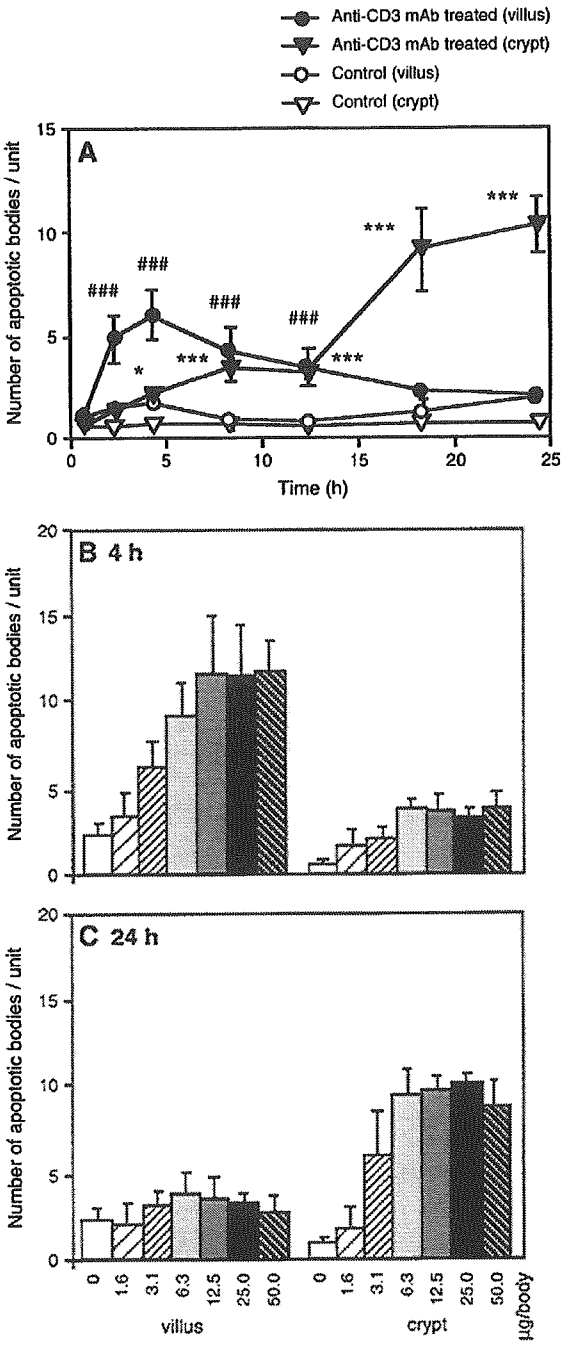

Fig. 1. Time course (A) and dose dependency (B, C) of anti-CD3-induced apoptosis in the jejunum of C3H/HeN mice. Control mice received saline alone. Data represent the means ± SD of apoptosis per villus per crypt unit. (A) The antibody was administered intraperitoneally at a dose of 12.5 μg per mouse (number of mice = 6–7). Apoptotic cells with condensing/fragmenting nuclei appeared in the small intestine bi-phasically. ### $P < 0.0005$ versus the control group (villus) and *$P < 0.05$; ***$P < 0.0005$ versus the control group (crypt) at each time. (B) Four hours after and (C) 24 h after antibody injection (number of mice = 5). Apoptotic cells with condensing/fragmenting nuclei arose dose dependently in the villus at 4 h (B) and in the crypt at 24 h (C).

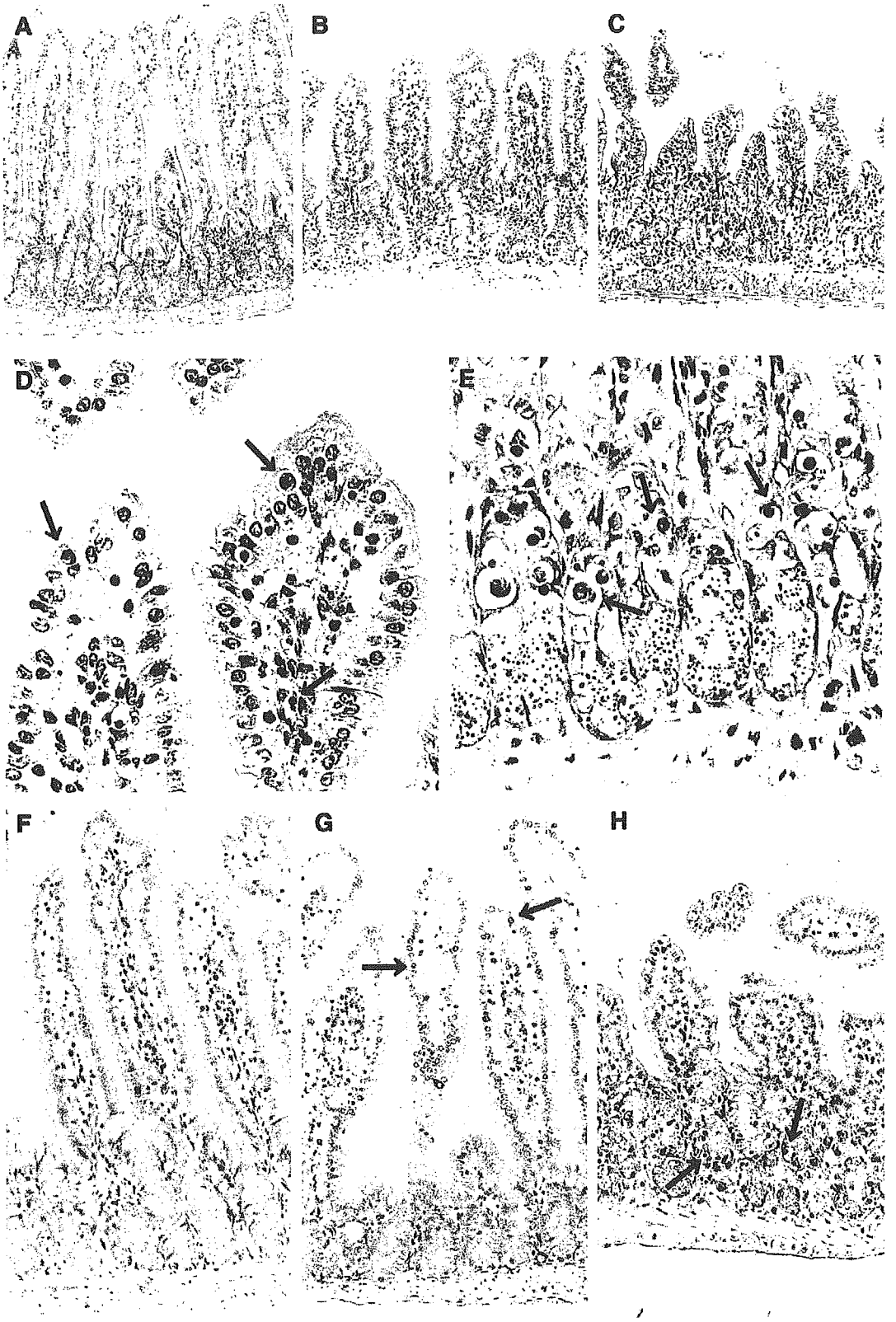
A
B
C
D
E
F
G
H

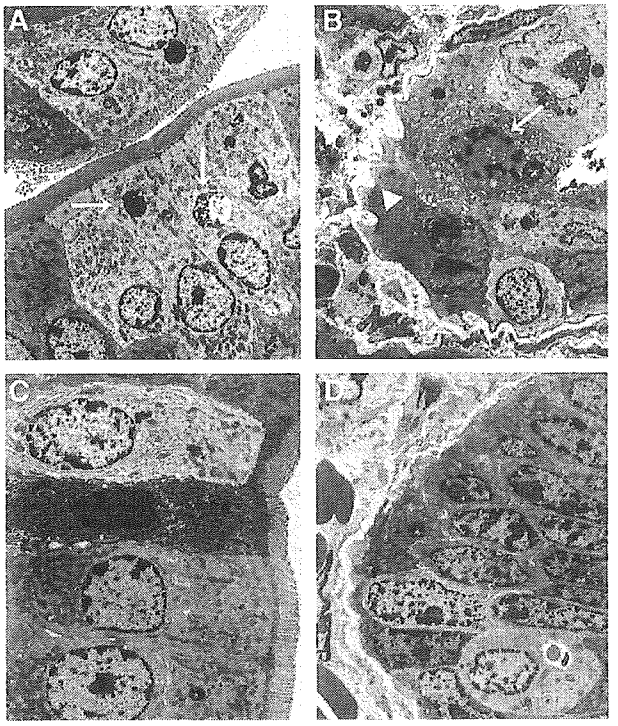

Fig. 3. Electron microscopic findings after anti-CD3 injection. (A) Condensed and fragmented nuclei (arrow) are seen in ciliated villous epithelial cells 4 h after anti-CD3 injection. The cytoplasm shows little change at this time. Neither apoptotic nor damaged lymphocyte infiltrate is observed. Little apoptosis occurs in IEL (unpublished observations in our laboratory). (B) Condensed and fragmented nuclei (arrow) and expanded mitochondria are seen in one crypt epithelial cell 24 h after anti-CD3 injection. The other crypt epithelial cells do not have typical condensed and/or fragmented nuclei, but nuclei are beginning to show damage. Neither apoptotic nor damaged lymphocyte infiltrate is present. The arrowhead indicates basal membrane. Little apoptosis occurs in lamina propria lymphocytes (unpublished observations in our laboratory). (C) Villus in naive mice and (D) crypt in naive mice. Naive mice have little apoptosis either in the villus or the crypt. The invasion of any microflora has not been observed in the small intestinal epithelia (A–D and unpublished observations). Original magnification: ×50 000.

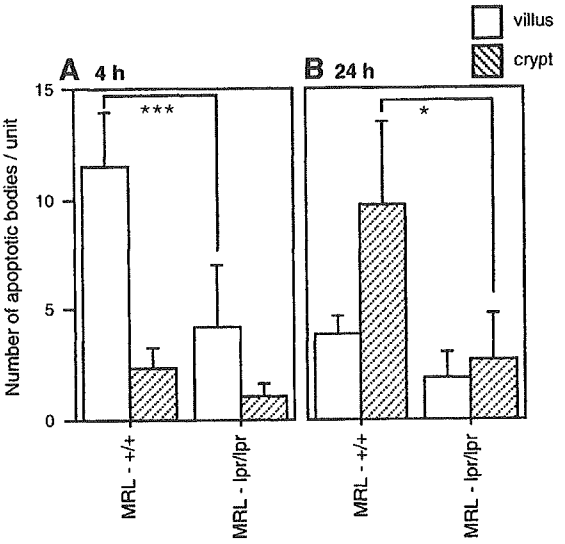

Fig. 4. Differences in the number of apoptotic cells in MRL-+/+ and MRL-*lpr/lpr* mice after anti-CD3 (12.5 μg per mouse) administered intraperitoneally. Apoptotic bodies with clearly fragmented and/or condensed nuclei, the most classical and definitive feature of apoptosis, were counted as described in *Histology* in Methods. Data represent the means ± SD of apoptotic cells per villus per crypt unit 4 (A) and 24 h (B) after antibody administration (number of mice = 3–5). The number of apoptotic bodies in mice administered saline instead of anti-CD3 was <1.5 for both strains. $*P < 0.05$; $***P < 0.0005$ versus the control group.

injection accompanied by intestinal injury, we analyzed *ex vivo* Fas-mediated cytotoxicity of these lymphocytes after anti-CD3 injection. At an E/T ratio of 1 : 20, freshly isolated IEL and SPL showed a weak spontaneous killing activity, with IEL stronger than SPL, but MLNC and PPL showed no detectable activity (Fig. 5A). When stimulated with anti-CD3 *in vitro*, cytotoxicity mediated by IEL and SPL was strongly induced, but was only marginally induced in MLNC and PPL, which is consistent with the data of Lin *et al.* (23) (Fig. 5B). Next, we analyzed the killer activity of lymphocytes isolated from mice injected with anti-CD3 antibody without *in vitro* stimulation (Fig. 5C). Similar to cells stimulated *in vitro*, the *in vivo* induction of cytotoxicity by anti-CD3 was mainly observed in IEL and SPL. The cytotoxicity of IEL increased rapidly and remained at the highest level from 0.5 to 4 h after the anti-CD3 injection and, thereafter, declined slowly. In contrast, SPL cytotoxicity rose more slowly, peaked from 4 to 8 h after the injection and then declined. The maximum cytotoxicities of IEL and SPL were similar to the maximum value obtained by *in vitro* stimulation, and the potency was IEL > SPL (approximately 60 versus 40% lysis at an E/T ratio of 1 : 20). The killer activity at 24 h was not analyzed because IEL were depleted by that time in this model. These results showed that the cytotoxicity of IEL and SPL was induced at different times and with different potency, which raised the possibility that IEL and SPL may be responsible for the induction of the different phases of IEC apoptosis.

We examined the expression of CD3, CD69, FasL and Fas on IEL and SPL from anti-CD3-treated and untreated mice (Fig. 6). FasL was constitutively expressed on IEL, but the number of $FasL^+$ cells increased slightly at 4 h after injection of anti-CD3 and returned to the normal levels by 24 h. On the other hand, FasL was expressed at a very low level on SPL of

Fig. 2. Histological sections of the jejunum of C3H/HeN mice. Anti-CD3 was administered at a dose of 12.5 μg per mouse. (A–E) H&E staining. (F–H) TUNEL assay. (A and F) Control mice receiving saline alone. (B, D and G) Four hours after the antibody injection. (C, D and G) Twenty-four hours after the antibody injection. Control mice have few apoptotic cells (A and F). Many apoptotic cells (arrow) are seen in the villus at 4 h (D and G) and in the crypt at 24 h (E and H) after anti-CD3 injection. Original magnification: A–C, ×25; D and E, ×132; F–H, ×50.